On The Role of Energy Deposition in Triggering SEGR in Power MOSFETs†

Luis E. Selva[1,2], Gary M. Swift[1], William A. Taylor[2], Larry D. Edmonds[1]
[1]Jet Propulsion Laboratory, California Institute of Technology
[2]Department of Physics and Astronomy, California State University Los Angeles

Abstract

Single event gate rupture (SEGR) was studied using three types of power MOSFET devices with ions having incident linear energy transfers (LETs) in silicon from 26 to 82 MeV·cm^2/mg. Results are: 1) consistent with Wrobel's oxide breakdown for V_{DS} = 0 volts (for both normal incidence and angle); and 2) when V_{GS} = 0 volts, energy deposited near the Si/SiO_2 interface is more important than the energy deposited deeper in the epi.

I. INTRODUCTION

A power MOSFET is a MOS (metal oxide semiconductor) device that regulates large current flow from the source to the drain by the application of a voltage to the gate. Key features of the device are the epitaxial layer, which is a doped semiconductor, and the silicon dioxide (SiO_2) insulating layer, which sits on top of the epi, designed to prevent gate current from crossing into the epi region. Energetic heavy ions that traverse the MOSFET structure can induce SEGR, which is a rupture of the gate oxide.

Researchers have, for several years, studied SEGR experimentally and reported several semi-empirical expressions describing their results. The semi-empirical expressions for critical gate voltage (V_{GS}), referred to as V_{CR} in this paper, has been expressed in the following form: $V_{GS} = G + F\cdot V_{DS}$, where both G and F are functions of LET (incident) or (as of 1998) of Z for the G term [1-4]. The G term has historically been associated with the gate oxide response (capacitor) and the F term with the epitaxial response (substrate) coupled with the oxide response.

Experiments conducted by Wrobel on dielectric structures (SiO_2 and SiO_2/Si_3N_4 composite capacitors) demonstrated that V_{CR} (for gate rupture) and LET in the dielectric medium have an inverse relationship along with an angular dependence that follows an inverse cosine relationship [5]. Wrobel proposed the following equation for the critical electric field for SEGR,

$$E_{CR}(\text{oxide}) = 4.1\text{x}10^7\cdot(1/\text{LET})^{1/2}\cdot 1/\cos(\theta+5°)\ [\text{MV/cm}] \quad (1)$$

Experimental results presented in this paper are consistent with an inverse LET dependence as well as an inverse cosine relationship, but do not clearly differentiate between the various models and fits proposed in the literature, including Wrobel's.

Titus, et al, have suggested that the mechanism governing SEGR might be a function of the total energy transferred [deposited] into the epitaxial layer [3]. The present paper presents experimental results, which investigated whether that conclusion could be extended to a select set of test ions with different Z's and varying energies. For this study, three devices with the similar oxides but with different epitaxial characteristics (doping and depth) were chosen. Results support the conclusion that energy deposited in the epitaxial contributes to oxide stress and rupture, with energy deposited nearer the Si/SiO_2 interface being more important.

II. BACKGROUND

The adopted test methodology was to select test devices with similar oxides, but different epitaxial doping profiles and depth. N-channel MOSFETs from International Rectifier were used as the test vehicles. The test devices used were the IR2N6782 (100V), IR2N6790 (200V), and IR2N6786 (400V), which have similar over layers and oxide structure but differing epitaxial depth and doping levels. The MOSFETs were irradiated with ions of several energies and varying Z (atomic number).

In addition to the irradiated devices, over 80 devices were electrically stressed (without ions), in order to determine silicon (Si) and gate oxide (SiO_2) breakdown points. Thirty-eight 100V devices, thirty-two 200V devices and fifteen 400V devices were utilized to determined electrical characteristics. Oxide breakdown was defined as the point where the gate to source current exceeded one µA. Oxide rupture was accomplished by holding V_{DS} constant, while stepping up V_{GS}. Breakdown for silicon was defined as the point where the drain to source current exceeded 100µA, effectively shorting out the region between the source and drain. Silicon breakdown tests were conducted by holding V_{GS} constant and stepping up V_{DS}. The time of application of each voltage step varied from ~0.5 - 3 seconds. Between voltage steps, the device was measured with V_{GS} set at specification maximum (20 volts) and V_{DS} = 0 volts, followed by V_{GS} = 0 volts and V_{DS} = specification maximum (100V, and 200V for both IR2N6790 and IR2N6786). If the transistor was still functional then the voltage was stepped up and the test continued. All electrical biasing and characterizations were performed with an HP4142B using three HP41420A source-measuring units (SMUs).

Silicon electrical breakdown without irradiation for the 100V device was measured at 126 volts with 90% of the parts failing within ± 5V of 126V, independent of V_{GS} (below breakdown); oxide breakdown was measured at −86V ± 15% for 90% of the parts, independent of V_{DS} (below breakdown). The breakdown values for the 200V devices were -85 volts for the oxide and 245 volts for the silicon with all measurements yielding identical values. Oxide breakdown for the 400V

†The work described in this paper was carried out by the Jet Propulsion Laboratory, California Institute of Technology, under contract with the National Aeronautics and Space Administration, Code AE. Work funded by the NASA Microelectronics Space Radiation Effects Program (MSREP).

0018-9499/99$10.00

devices were measured at –74V ± 3%. Silicon breakdown points were not obtained for the 400V devices.

The selected ions and incident energies were Br^{79} (Z = 35, 276 MeV), I^{127} (Z = 53, 350 MeV) and Ni^{58} (Z = 28, 266 MeV) obtained at the Brookhaven National Laboratory (BNL) Tandem van de Graaff. Longer range ions were Xe^{129} (Z = 54, 1961 MeV), Nb^{93} (Z = 41, 1030 and 907 MeV), and Au^{197} (Z = 79, 2068 MeV) from the Texas A&M Cyclotron Institute. Short-range ions produced as fission fragments spontaneously emitted from a Californium (Cf^{252}) source were also used.

Assignment of a representative Cf^{252} fission fragment is somewhat problematic. Californium-252 spontaneously fissions into two main asymmetric fragments with a distribution of energies and atomic numbers. In all cases, the fragments have lower energy than that of the Bragg peak, so that LET always declines as they slow down. Although starting out with similar LETs to the lighter ions, the heavier fragments (higher Z) have more rapidly declining LET and less penetration. Thus, for SEGR onset biases, only the lighter fragments need be considered. Fortunately, the kinematics of the fission process [6] are such that the distribution of LETs of light fragments is narrower than either the Z distribution or the energy distribution. For example, 100 MeV Mo^{103} (Z=42) has an incident LET of 44.8 MeV cm^2/mg in silicon, while 112 MeV Pd^{113} (Z=46) has an LET = 47.9. Thus, the most likely fragment Ru^{108} (Z=44) with an average energy of 105.7 MeV (LET=46.5) is a good representative choice. Note that an extreme case fragment, 110 MeV Cd^{120} with an LET of 49.1, can be expected about once per cm^2 for these irradiations (fluence of 1×10^5 ions/cm^2). Thus, 105.7 MeV Ru^{108} was selected as the most representative ion from the Cf^{252} source. Large error bars on its LET are shown to cover the distribution of fission fragments produced, as in figure 5.

The oxide and dead layer thickness for each device type was determined by using a scanning electron microscope (SEM) with a magnification of 2000X. The measured oxide and dead layer thickness were 71 ± 8nm and 4.3 ± 0.3µm, respectively for all three-device types. The dead layer thickness was converted to a silicon equivalence of 4.5 ± 0.5µm, in order to correct for energy lost before the ion penetrated the insulator. Doping levels and epitaxial depth were obtained from spreading resistance measurements conducted at an independent laboratory and are as follows: 3×10^{15} ions/cc and 15µm, 1×10^{15} ions/cc and 26 µm, and 4×10^{14} ions/cc and 40µm for the 100V, 200V, and 400V devices, respectively.

III. Experimental Results

A. *Critical SEGR contours*

Critical SEGR contours are measured as minimum bias pairs of V_{DS} and V_{GS} for a given ion with a particular incident energy. There is a different curve for each incident ion-energy condition. For any ion, any point (V_{DS}, V_{GS}) on the contour is an onset condition for SEGR. The critical SEGR contours for IR2N6782 (100V), IR2N6790 (200V) and IR2N6786 (400V) devices are shown in figures 1, 2 and 3. The solid curves in each figure are a smooth fit of the computed average of last pass and failure voltage. Each data point consists of a pair of minimum bias conditions (gate to source voltage, $|V_{GS}|$, and drain to source voltage, V_{DS}) at which SEGR occurred. Gate rupture was defined to have taken place at the minimum V_{DS}, $|V_{GS}|$ bias conditions for a particular ion beam energy. For a given test either $|V_{GS}|$ or V_{DS} was increased in steps, while the other was maintained fixed. At each bias step the device was irradiated with a fluence of 1×10^5 ions/cm^2 or until SEGR. Flux was maintained at about 1×10^4 ions/cm^2 per second producing roughly ten second runs, except in the Cf^{252} irradiations where the runs were ~ 30 minutes.

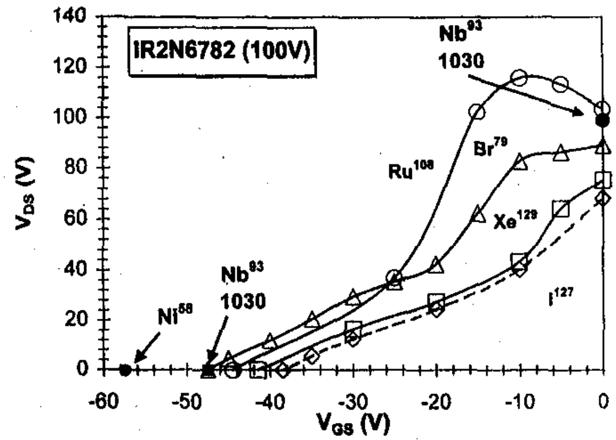

Figure 1: SEGR contour curves for IR2N6782 (100V).

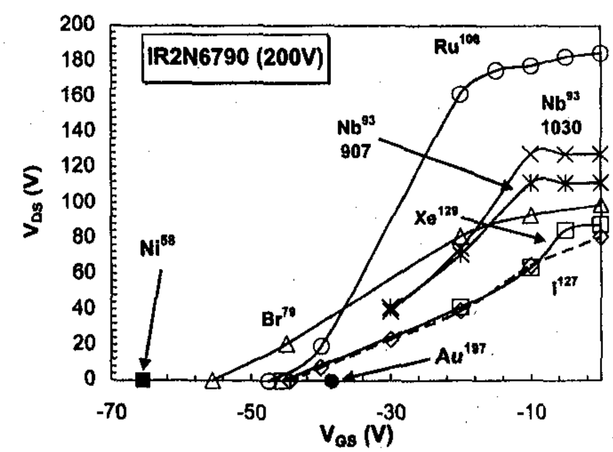

Figure 2: SEGR contour curves for IR2N6790 (200V).

Between irradiations, the device was measured with V_{GS} = specification maximum (-20 volts) and V_{DS} = 0 volts followed by V_{DS} = specification maximum (100V and 200V for both IR2N6790 and IR2N6786) and V_{GS} = 0 volts. If the transistor was still operational, the voltage was stepped up and the device irradiated again. All devices were biased and measured with a Hewlett-Packard HP4142B using three HP41420A SMUs.

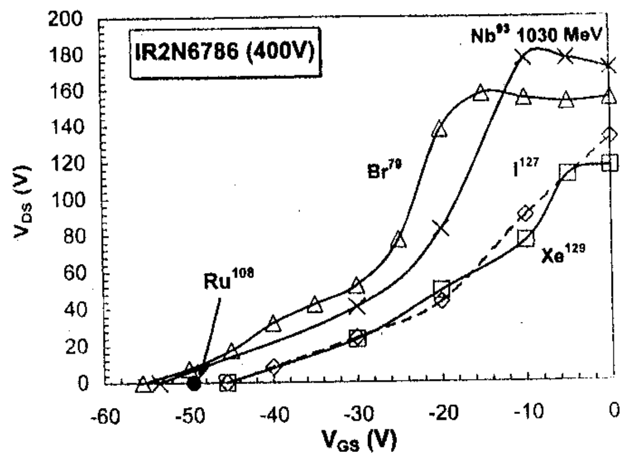

Figure 3: SEGR contour curves for IR2N6786 (400V).

B. Oxide Response

Table 1 combines the results for all 3 transistor types and ranks the ions on oxide SEGR efficiency (at V_{DS} = 0 volts) based on the experimental observations from figures 1 - 3. Utilizing the energy-range tables from SRIM/TRIM for each ion, table 1 shows the expected energy deposited in the oxide region for the three types of power MOSFETs, for a 4.5μm silicon-equivalent dead layer above the oxide and an oxide thickness of 75nm.

Table 1.
Ranking of Oxide SEGR Efficiency

Ranking of Ions (MeV)	Energy deposited in Oxide (MeV)	LET SiO_2 (MeV cm^2/mg)	V_{CR} (Volts) (calculated from (1))	Z	Incident LET Si
1) Au^{197} 2068	1.62	98.3	31.1	79	86.6
2) I^{127} 350	1.19	72.2	36.2	53	61.8
3) Xe^{129} 1961	0.88	53.5	42.1	54	47.5
4) Ru^{108} 105.7	0.76	46.1	45.7	44	46.0
5) Br^{79} 276	0.75	45.2	45.8	35	38.1
6) Nb^{93} 1030	0.67	40.7	48.3	41	35.3
7) Ni^{58} 266	0.52	31.7	54.7	28	26.6

The ions listed in column 1 are ranked in order of oxide SEGR efficiency. This ranking is from figures 1 - 3. That is, Au^{197} (2068 MeV) is the ion (of the test ions used) most capable of causing SEGR at lowest $|V_{GS}|$ when V_{DS} = 0 volts. Column 2 is a tabulation of the calculated energy deposition in the oxide by each ion with an error of 1.5% or less based on the 0.5μm uncertainty in dead layer thickness. Column 3 is the computed average linear energy transfer (LET) in the silicon dioxide layer. LET is defined as the energy deposited per path length divided by the density of the material. Silicon is a denser material than silicon dioxide, thus values in column 3 are generally larger than for column 5, except for Ru^{108} which losses ~ 43% of its initial kinetic energy to the dead layer. Because the oxide is relatively thin and the energy deposition (ΔE) is proportional to LET in the oxide, i.e., $\Delta E \propto$ LET(SiO_2). Column 4 is the expected V_{CR} value as determined by equation 1 for a 75nm oxide, with the cosine term set to 1. Note, all data points in table 1 were obtained from irradiations at $\theta = 0°$. Column 5 is the atomic number Z for each atom used. Lastly, column 6 is the LET (Si) incident on the dead layer.

Observe the correlation between columns 1, 2, 3, 4, and 6. Note that the ranking of column 3 implies the ranking of column 4 (and vice-versa) via equation 1, so the two columns are equivalent but different units of measure. Note that the 75nm oxide thickness was incorporated into equation 1 to convert electric field to voltage. Both of these columns agree with the measured ranking shown in column 1. Column 5 does not rank [order] the ions as effectively as the other parameters. Iodine (I^{127} Z=53) and bromine (Br^{79} Z=35) appear to be out of order. Notice that it appears that incident LET(Si), column 6, works well as an indicator of SEGR efficiency, however, this results from the thin over layer. If the oxide were located deeper in the device, incident LET and energy deposited in the oxide would not correlate as well with each other. In other words, incident LET works well as an indicator of SEGR efficiency only when the oxide is near the top of the structure, that is before the ion has had time to lose some of its kinetic energy before reaching the oxide.

Figure 4 plots energy deposited in the form of LET(SiO_2) for each ion used in all three device types as a function of critical gate voltage (V_{CR} for $|V_{GS}|$) with V_{DS} = 0 volts. The 200V and 400V data appear to be shifted away from the 100V data. This result is presently not understood.

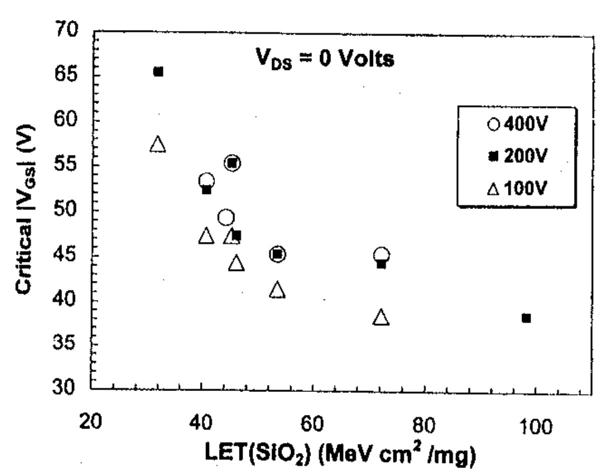

Figure 4: Critical Gate Voltage (V_{CR}) vs. LET(SiO_2) proportional to energy deposition for all device types.

Figure 5 is a plot of the 100V data with the addition of the Wrobel equation (1) as curve A an alternative equation was introduced by Titus et al. in 1995 [2] as curve B:

$$V_{CR}=50/(1+LET/53) \qquad (2)$$

Notice that both the Wrobel and the Titus equation fit the 100V data. For the Wrobel equation, no fitting parameter was used. However, the Titus LET [1] and Z [4] equations require two fitting parameters. For the LET equation (2), the adjustable parameters were adjusted from 53 to 55 and 50 to 85 to improve the fit with the present data; this is shown as curve B. Curve A is inverse square-root dependent in LET while B is inversely dependent on LET. Future experiments may help discriminate between these two equations. Particularly by exploring the LET(SiO_2) range between 10 to 35 MeV cm^2/mg with the 100V device or with a similar MOSFET structure. At this time, the Wrobel formulation is preferable because it requires no adjustments to fit the present data. Furthermore, Wrobel gives a physical argument for this form. Note, however, it is clearly inapplicable at very low LETs where it predicts gate biases higher than the electrical (no ion) rupture values.

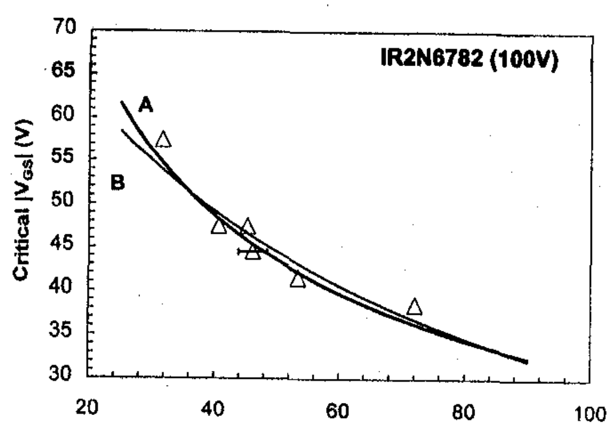

Figure 5: Critical Gate Voltage (V_{CR} = $|V_{GS}|$) vs. LET(SiO_2) proportional to energy deposition for IR2N6782 (100V).

C. Oxide Response: Angular Dependence

The angular dependence is plotted in figure 6 for the 100V device. In the figure, the critical gate voltage (V_{CR} = $|V_{GS}|$) is plotted versus the ion's angle of incidence. Curve A is generated by the angular component of the Wrobel equation (1), which includes an angle offset of 5°. Curve B is generated by a $1/\cos\theta$ factor and curve C is generated by a $(1/\cos\theta)^{0.7}$ as was obtained by Titus et al [2]. Based on the data plotted in figure 6, the best fit curve is B, which is the Wrobel equation but without the angle offset.

D. Epitaxial Response

In table 2, columns 1 through 3 tabulate the epitaxial characteristics of the three MOSFETs. The ions listed in column 4 are ranked in order of epitaxial SEGR efficiency. For example Iodine (I^{127} 350 MeV) is the ion (of the test ions used) most capable of inducing SEGR at the lowest V_{DS} when V_{GS} was set to zero volts for the 100V and 200V devices, figures 1 and 2, respectively. In the 400V device Xe^{129} is more effective than I^{127} in causing SEGR, according to the experimental results in figure 3. SRIM/TRIM tables were employed to calculate the range and energy deposited in the epitaxial by the various ions listed in columns 5 and 6. Column 6 is a list of the calculated total energy deposition in the epitaxial after the ion has traversed the dead layer and silicon dioxide insulator. Column 7 is a list of the weighted average LET(Si) for the particular ion and for the given epitaxial depth. Information as to how this parameter was computed is given later in this section. Columns 8 and 9 list the experimental results for the bias conditions to trigger SEGR when V_{DS} = 0 volts and for V_{GS} = 0 volts, respectively. The ion rankings in column 4 are based on column 9. Column 10 is a list of the atomic number Z for each ion used. Lastly, column 11 is a list of the LET(Si) incident on the dead layer.

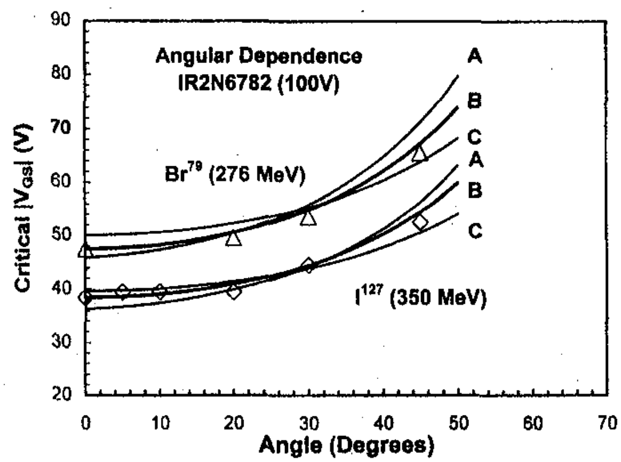

Figure 6: Oxide angular dependence, V_{CR} versus angle of incidence for IR2N6782 (100V).

Note the correlation between columns 4, 6, 7, and 9 for the 100V device. For the 200V device columns 4, 7 and 9 correlate well. For the 400V device columns 4, 7, and 9 correlate well. Column 6, energy deposition in the epitaxial by the ion, works as an indicator of epitaxial SEGR efficiency for the thinner epitaxial (100Vdevice) but not for the 200V and 400V devices. The atomic number Z does not correlate in all cases with the ion ranking in column 4. Incident LET(Si) works well as an indicator of SEGR efficiency for ions whose range exceeds the length of the epitaxial depth. For ions that stop in the epi, e.g., Ru^{108} in all devices and, I^{127} and Br^{79} in the 400V device, the incident LET does not rank these ions as observed in column 4. Weighted average LET is (column 7) the only parameter in table 2 that ranks all ions for all devices in accordance with the observed SEGR data of column 9.

Table 2.
Ranking of Epitaxial SEGR Efficiency

Device Type (1)	Doping (ions per cm^3) (2)	Epi depth (μm) T_e (3)	Ranking of Ions (MeV) (4)	Ion Range (μm) (5)	Energy deposited (MeV) in Epi (6)	Weighted Ave. LET (MeV cm^2/mg) (7)	Critical ($\lvert V_{GS}\rvert$) at V_{DS}=0 volts (8)	Critical (V_{DS}) at V_{GS}=0 volts (9)	Z (10)	LET(Si) Incident (MeV cm^2/mg) (11)
IR2N6782 100V	$3.0x10^{15}$	15	1) I^{127} 350	33.0	202	60.6	38.5	68.5	53	61.8
			2) Xe^{129} 1961	158.4	169	48.9	41.5	75.5	54	47.5
			3) Br^{79} 276	33.6	138	39.8	47.5	84.5	35	38.1
			4) Nb^{93} 1030	111.4	128	36.8	47.5	99.0	41	35.3
			5) Ru^{108} 105.7	12.7	60	25.8	44.5	103.5	44	46.5
IR2N6790 200V	$1.0x10^{15}$	26	1) I^{127} 350	33.0	277	57.3	44.5	80.5	53	61.8
			2) Xe^{129} 1961	158.4	297	49.1	45.5	87.5	54	47.5
			3) Br^{79} 276	33.6	213	39.3	55.5	99.0	35	38.1
			4) Nb^{93} 907	96.7	235	38.5	Not done	111.5	41	36.7
			5) Nb^{93} 1030	111.4	225	36.9	52.5	127.5	41	35.3
			6) Ru^{108} 105.7	12.7	60	19.4	47.5	186.0	44	46.5
IR2N6786 400V	$4.0x10^{14}$	40	1) Xe^{129} 1961	158.4	466	49.4	45.5	117.5	54	47.5
			2) I^{127} 360	33.0	284	48.7	45.5	133.0	53	61.8
			3) Br^{79} 276	33.6	220	34.8	55.5	155.0	35	38.1
			4) Nb^{93} 1030	111.4	353	37.3	53.5	171.5	41	35.3
			5) Ru^{108} 105.7	12.7	60	14.2	49.5	Not done	44	46.5

Three fitting (weighted) functions were tried, one linear in depth, one quadratic in depth and one cubic in depth. The best fit was obtained using the quadratic weighted function, which is given in equation (3). This function weighs energy deposited nearer the Si/SiO_2 interface more heavily than energy deposited deeper in the epi. Equation (4) is the weighted average LET, <L>, where Te is the epi thickness, and x is the ion distance below the Si/SiO_2 interface.

$$\omega(x)=\left(\frac{Te-x}{Te}\right)^2 \tag{3}$$

$$\langle L\rangle=\frac{\int_0^{Te}\omega(x)LET(x)dx}{\int_0^{Te}\omega(x)dx} \tag{4}$$

Results of the calculations using the above equations are listed in table 2 column 7.

The weighted average LET ranked all the ions for all three device types in the same order as column 9. This includes ions with the same Z like the Niobium 907 and 1030 MeV and ions with similar Z like Iodine and Xenon, even though these two ions have widely different energies, 350 and 1961 MeV. Long range, intermediate and short-range ions were also ranked correctly by the weighted average LET function. For the results presented here, energy deposited near the Si/SiO_2 interface is more important in causing SEGR than energy deposited deeper in the epi.

IV. Numerical Results

Computer simulation results, like those of reference 7, give insight into how the energy deposited by the passage of an energetic heavy ion can induce a high transient electric field across the oxide. The effects of a 40μm ion track incident on a virtual power MOSFET were studied with computer simulation using the two-dimensional code PISCES.

PISCES was converted to cylindrical coordinates and was used to solve drift/diffusion equations subject to the usual physics (bandgap narrowing, Shockley-Read-Hall and Auger recombination, and mobilities depending on doping density and on the electric field), except for carrier-carrier scattering or avalanching. PISCES allows the user to input a low-concentration lifetime and then PISCES modifies this lifetime to account for doping density. The input lifetime was arbitrarily chosen to be 1μs. The simulated ion track density was arbitrarily chosen to be longitudinally uniform over the track length and have a gaussian radial distribution with a 0.5μm characteristic radius.

The baseline case for the simulation was an ion with a constant LET of 40 MeV·cm^2/mg. The energy deposited by the ion was assumed to have been deposited instantaneously prior to the commencement of the simulation. The baseline case was a power MOSFET structure with an oxide thickness of 46nm, an epi depth of 19μm, an epi doping level of 3×10^{15} ions/cc, a substrate doping level of 1×10^{16} ion/cc, a substrate depth of 21μm, and biased with $V_{GS}=0$ and $V_{DS}=100$ volts. Three cases were studied using a single variation away from the baseline case, thus a total of 4 cases were studied. First, the doping level was lowered in the epi to 1×10^{15} ions/cc. Second, the gate bias was set to V_{GS} = -10 volts. Third, the ion track was shortened so that it terminates in the epi at 8μm below the Si/SiO_2 interface. Table 3 summarizes the peak value of the transient electric field and the time to reach this peak for the 4 cases studied.

Table 3.
Peak electric field strength in the oxide for each case study based on PISCES (computer simulation).

Case studies 1 through 4	Electric Field (MV/cm)	Time to peak (picoseconds)
1) Baseline	13.6	3.92
2) Lower doping	11.2	5.00
3) V_{GS} = -10 volts	14.5	4.01
4) Short ion track	12.1	2.88

Comparison between cases 1 and 2 show the effects of doping on the peak electric field. Lower doping in the epi produces a smaller peak transient electric field following the passage of an energetic ion. Thus, for a highly doped epi the critical voltage for SEGR would be lower than for a lower doped epitaxial. All of the data in table 2 are consistent with this result.

Comparison of cases 1 and 3 highlights the role of the applied bias across the oxide. Increasing the voltage between the gate and source (V_{GS}) enhances the transient electric field across the oxide. Thus it is reasonable to expect that lower V_{DS} values are needed to induce SEGR for larger critical gate voltage ($|V_{GS}|$) values. This is consistent with the results in figures 1 – 3.

Comparing cases 1 and 4, one can conclude that the track segment nearest the Si/SiO_2 interface is more important than those further away in inducing SEGR. This is consistent with the weighted average LET conclusion mentioned previously. Notice that the 8μm track obtains a peak electric field of 12.1 MV/cm where as the longer 19μm track achieves 13.6MV/cm.

According to the results of case 4, the first 8μm of the baseline case achieved its peak value at 2.88ps. The additional 32μm of ion track only increased the electric field by 1.5MV/cm and shifted the time to peak field by an additional 1.04ps. Based on ion traversal time studies found in table 4, ions take on the order of picoseconds to travel through the entire MOSFET. Thus it is not reasonable to assume instantaneous ion traversal. These similar time frames may contribute to the observation that energy deposited near the Si/SiO2 interface is more important in inducing SEGR.

Table 4.
Calculated ion traversal time (picoseconds) based on SRIM/TRIM tables.

Ion (MeV)	4.5μm Si dead layer	Oxide (75nm)	Epi 100V 15μm	Epi 200V 26μm	Epi 400V 40μm
Au^{197} 2068	0.10	0.0018	0.35	0.63	1.02
Xe^{129} 1961	0.08	0.0015	0.28	0.50	0.79
Nb^{93} 1030	0.10	0.0017	0.34	0.60	0.97
Nb^{93} 907	0.10	0.0019	0.36	0.65	1.06
I^{127} 350	0.20	0.004	0.94	2.64	4.15*
Br^{79} 276	0.18	0.0035	0.79	2.07	3.63*
Ni^{58} 266	0.15	0.0055	0.54	0.98	1.63
Ru^{108} 105.7	0.37	0.0078	2.89*	2.89*	2.89*

* = stops within the epitaxial layer

V. Conclusion

SEGR is a phenomenon that is driven by energy deposition and applied electric field. For $V_{DS} = 0$ Volts the SEGR results presented here are consistent with capacitor studies by Wrobel [5] and with MOSFET studies [1 – 4].

When the power MOSFET was biased with $V_{GS} = 0$ Volts, energy deposited in the epitaxial layer plays an important role in triggering SEGR. The failure voltage (V_{DS}) is inversely proportional to the average weighted LET; similar to the results found for capacitor like behavior. The weighted function utilized has the property that the energy deposited near the Si/SiO_2 interface is more important in inducing SEGR than energy deposited deeper. Even though energy deposition near the oxide is favored, energy deposited deeper in the device does affect SEGR.

Computer modeling showed that the transient electric field generated in the oxide is sensitive to epi doping level, ion track range, and biasing conditions. Simulation results are consistent with the experimental results. The time to peak transient electric field was found to be on the order of time that it takes for the ion to traverse the entire MOSFET. Current computer modeling assumes an instantaneous energy deposition by the ion. Computed transient electric fields may be too high.

Acknowledgments

The authors would like to thank the following individuals for their time and effort in assisting in data gathering and in generating computer programs, which facilitated in the analysis of the SEGR data: Steven M. Guertin and Tetsuo F. Miyahira.

References

[1] C. F. Wheatley, J. L. Titus, D. I Burton, "Single-Event Gate Rupture in Vertical Power MOSFETs; An Original Empirical Expression," *IEEE Trans. Nucl. Sci.*, NS-41, No. 6, pp. 2152-2159, 1994.

[2] J. L. Titus, C. F. Wheatley, D. I. Burton, I. Mouret, M. Allenspach, J. Brews, R. Schrimpf, K. Galloway and R. L. Pease, "Impact of Oxide Thickness on SEGR in Vertical Power MOSFETs; Development of a Semi-Empirical Expression," *IEEE Trans., Nucl. Sci.*, vol. 42, No. 6, pp. 1928-1934, 1995.

[3] J. L. Titus, C. F. Wheatley, M. Allenspach, R. D. Schrimpf, D. I. Burton, J. R. Brews, K. F. Galloway and R. L. Pease, "Influence of Ion Beam Energy on SEGR Failure Threshold of Vertical Power MOSFETs," *IEEE Trans. Nucl. Sci.*, vol. 43, No. 6, pp. 2938-2943, 1996.

[4] J. L. Titus, C. F. Wheatley, K. M. Van Tyne, J. F. Krieg, D. I. Burton and A. B. Campbell, "Effects of Ion Energy Upon Dielectric Breakdown of the Capacitor Response in Vertical Power MOSFETs," *IEEE Trans. Nucl. Sci.*, NS-45, No. 6, pp. 2492-2499, 1998.

[5] Theodore. F. Wrobel, "On Heavy Ion Induced Hard-Errors in Dielectric Structures," *IEEE Trans. Nucl. Sci.*, NS-34, No. 6, pp. 1262-1268, 1987.

[6] Earl K. Hyde, "The Nuclear Properties of the Heavy Elements III Fission Phenomena," Prentice-Hall, Inc., pp. 157-210, 1964.

[7] M. Allenspach, I. Mouret, J. L. Titus, C. F. Wheatley, Jr., R. L. Pease, J. R. Brews, R. D. Schrimpf and K. F. Galloway, "Single-Event Gate-Rupture in Power MOSFETs: Prediction of Breakdown Biases and Evaluation of Oxide Thickness Dependence," *IEEE Trans. Nucl. Sci.*, vol. 42, No. 6, pp. 1922-1927, 1995.